Applied Thermal Engineering 58 (2013) 291–297

Contents lists available at SciVerse ScienceDirect

Applied Thermal Engineering

journal homepage: www.elsevier.com/locate/apthermeng

Enhanced flow boiling in parallel microchannels with metallic porous coating

Pengfei Bai [a,*], Tao Tang [b], Biao Tang [a,*]

[a] School of Information and Optoelectronic Science and Engineering, South China Normal University, Guangzhou 510006, China
[b] Key Laboratory of Surface Functional Structure Manufacturing of Guangdong Higher Education Institutes, South China University of Technology, Guangzhou 510640, China

HIGHLIGHTS

- The enhanced flow boiling in porous-coated parallel microchannels was studied.
- The pressure drop and flow boiling instability performances were discussed.
- A size-dependant heat transfer enhancement from porous coatings was recorded.
- The mitigation of flow boiling instability by the porous coatings was observed.

ARTICLE INFO

Article history:
Received 4 December 2012
Accepted 27 April 2013
Available online 7 May 2013

Keywords:
Parallel microchannels
Flow boiling
Heat transfer
Pressure drop
Porous coating

ABSTRACT

Three heat sinks with porous-coated parallel microchannels were fabricated by using a solid-state sintering method. The enhanced flow boiling of anhydrous ethanol in the porous-coated microchannels was systematically studied and compared to that of bare microchannels. The changes in pressure drop, flow boiling instability and flow boiling heat transfer performances caused by the introducing of porous coatings were discussed. The effect of particle size on pressure drop and heat transfer performance was also studied. The porous-coated microchannels showed significant mitigation of flow boiling instability, which was explained by the changes in bubble dynamics. Dramatic enhancement of flow boiling heat transfer in the porous-coated microchannels was obtained. The enhancement from porous coatings showed dependence on particle size and diminished with the increase of vapor quality.

1. Introduction

Micro-channel flow boiling systems have shown promising prospects in applications demanding high-flux heat dissipation because of their compact sizes and effective heat transfer ability coming from latent heat of phase change. Since the first study on flow boiling in microchannels conducted by Tuckerman and Pease [1] in 1981, a number of works have been reported on this subject [2–6]. A comprehensive review covering the history, advances and challenges in flow boiling heat transfer in microchannels was given by Kandlikar [7]. Generally, the heat transfer coefficient, flow boiling instability and critical heat flux (CHF) are identified as the major concerns of flow boiling in microchannels. Developing micro-channel flow boiling systems which may provide both high performance of heat transfer and reliable system operation is always a challenge for the application of this technology.

With the development of boiling enhancement technology, many surface structures have been investigated in pool boiling experiments and shown great improvement of heat transfer performances [8,9]. The achievements in pool boiling heat transfer motivated the studies on the flow boiling in microchannels with enhanced structures.

Wang et al. [10] investigated the flow boiling heat transfer in vertical narrow channel with sintered aluminum powder surface. The flow pattern in the narrow channel was also observed by naked-eye. They found that the dominant flow pattern in the narrow channel is annular flow pattern with liquid guttae. An enhancement of 2–5 times in boiling heat transfer coefficient was obtained by introducing the porous surface in the flow channels. Wu et al. [11] reported a porous-coated surface with vapor channels and investigated the effects of size and density of the vapor channels on the boiling heat transfer. Krishnamurthy and Peles [6] studied the subcooled and low quality saturated flow boiling

* Corresponding authors. Tel.: +86 20 87114634.
E-mail addresses: deer_phil@yahoo.com.cn (P. Bai), yuezique@yahoo.com.cn, btang9@asu.edu (B. Tang).

1359-4311/$ – see front matter © 2013 Elsevier Ltd. All rights reserved.
http://dx.doi.org/10.1016/j.applthermaleng.2013.04.067

across micro pin fins entrenched in a microchannel under various mass fluxes and heat fluxes. The thermal performance evaluation comparison with a plain microchannel revealed that the presence of pin fins considerably enhanced the heat transfer coefficient. Khanikar et al. [12] studied the flow boiling characteristics in rectangular microchannels with carbon nanotubes (CNTs) coating and obtained a modest enhancement of heat transfer. The increase of pressure drop resulted from CNT coating was also observed, especially at high mass velocities.

Kandlikar et al. [5] studied the effects of artificial nucleation cavities and the pressure drop elements of different area reduction ratios on flow boiling stability. They found fabricated nucleation sites in conjunction with the 4% area pressure drop elements completely eliminated the instabilities associated with the reverse flow. Kuo et al. [13] also found the ability of reentrant cavities to suppress flow boiling oscillations and instabilities in microchannels. They suggested that, for the reentrant cavity devices, the reduced superheat and pressure at the initial stage of the bubble nucleation delayed and moderated the flow oscillation, and, thus, extended the stable boiling region and increased the CHF.

The previous studies imply that the flow boiling performance in microchannels can be improved by enhanced surface structures with some success. However, the knowledge of flow boiling characteristics from porous surfaces in microchannels is rather fragmentary. Particularly, the pressure drop and flow boiling instability in porous-coated microchannels were rarely studied.

Porous metallic coating is considered to be the most viable technique for the enhancement of boiling heat transfer, which can be formed by sintering, brazing, flame spraying, forming or electrodeposition [8]. Microporous coating was early proposed by O'Connor and You [14] and further developed by Chang and You [15]. The coating technique increases vapor/gas entrapment volume and active nucleation-site density by forming openly connected porous structures with cavities of different sizes, which significantly affects the nucleate boiling heat transfer because of the numerous embryonic bubbles in the unique microporous structures. Rainey and You [16] developed a unique "double enhancement" technique which combined a large-scale area enhancement (square pin-fin array) and a small-scale surface enhancement (microporous coating) for the enhancement of boiling heat transfer. The nucleate boiling and CHF behaviors were found to be the results of multiple, counteracting mechanisms: surface area enhancement, fin efficiency, surface microstructure (active nucleation site density), vapor bubble departure resistance, and re-wetting liquid flow resistance.

In the present study, the enhanced flow boiling of anhydrous ethanol in parallel microchannels with metallic porous coatings is systematically studied. The pressure drop, flow boiling instability and flow boiling heat transfer performances of the porous-coated microchannels are investigated and compared to those of bare microchannels. The effect of particle size on pressure drop and heat transfer performances is also discussed. Only part of the nucleate boiling region is studied. The critical heat flux (CHF) of the flow boiling in microchannels is not studied due to limited heating power.

2. Experimental methods

2.1. Preparation of micro-channel heat sinks

Three porous-coated micro-channel samples (named as #1, #2 and #3) and a bare micro-channel sample (named as #0) were prepared in this experiment. The parallel rectangular microchannels were fabricated by using EDM wire cutting process. A solid-state sintering technology (Fig. 1(a)) was employed to fabricate a metallic porous coating in the bottom of the microchannels. The porous coatings which were uniformly dispersed in samples #1, #2 and #3 were composed of dendrite copper powders with diameters of about 30, 55 and 90 μm, respectively. The sintering process was conducted at 900 °C for 30 min under the protection of nitrogen and hydrogen. The thickness of the porous structure was about 0.12 mm, which was controlled by a sintering mold (Fig. 1(b)). By using this method, the four samples sharing the same hydraulic diameter D_h of 0.54 mm were obtained.

2.2. Experimental setup

Fig. 2(a) depicts the construction of the test module employed in this study. The test module consists of a copper micro-channel heat sink, a polycarbonate cover, a copper heating block and two cartridge heaters (300–500 W). The heat sink was fixed firmly in the slot on the heating block which was placed in the epoxy base and insulated by asbestos around. As shown in Fig. 2(b), the platform surface of the heat sink is of 17 mm in width and 46 mm in length. Fifteen microchannels of 400 μm in width, 900 μm in depth and 32 mm in length are uniformly arrayed in an area of 10.8 × 32 mm on the heat sink. The temperature distribution along the axial direction of the heat sink was recorded by six uniformly installed K-type thermocouples, named K_0, K_1, K_2, K_3, K_4 and K_5, respectively. The details of the location of the six thermocouples are shown in Fig. 2(b).

Fig. 3 shows the experimental setup and the flow loop that delivers working fluid to the test module at the desired flow rate, inlet temperature and pressure. A micro-pump drives the working liquid from the loop's reservoir into a filter, followed by a volumetric flow meter, a water bath with temperature controller, and a fluid valve before entering the test module. The heating power of the test module was supplied by an adjustable autotransformer and monitored by a power meter. A compact condenser was situated downstream to cool the fluid passing through the test section. The temperature of the working fluid was measured at the inlet and outlet collectors of the test module, by two K-type thermocouples (K_{in} and K_{out}). The flow rate of the working fluid was controlled by adjusting the speed of the micro-pump and was monitored by a flow meter. A differential pressure transducer (DP1300, Senex, Guangzhou) was used to monitor the pressure drop between the inlet and the outlet of the test module. The pressures at the inlet and the outlet of the test module were also measured by two silicon pressure sensors, with sensitivity of 2.9 mV/kPa, response time of 3.0 ms. A microscope with 40× magnification was installed for observing the flow boiling process in microchannels. The data of temperatures and pressures were collected by a data acquisition system (Agilent 34970A, Agilent Technologies, Shanghai).

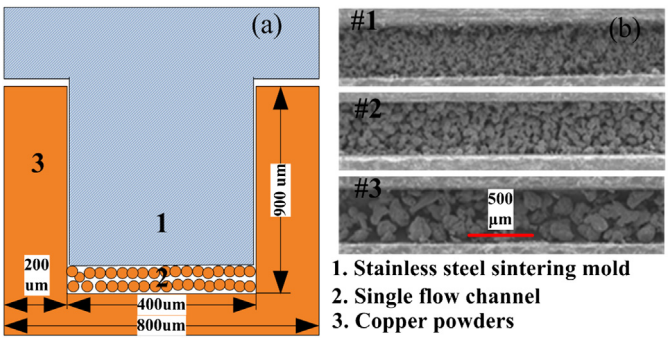

Fig. 1. (a) Schematic of solid-state sintering process (b) SEM images of porous-coated microchannels (#1, #2 and #3).

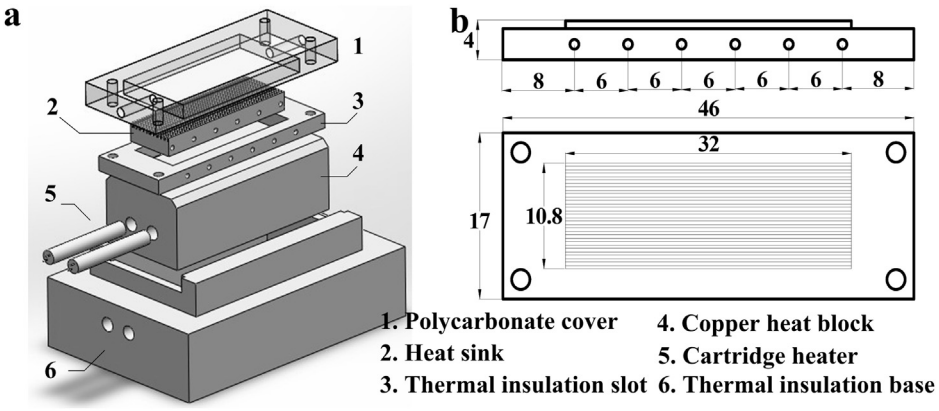

Fig. 2. Schematic of test module and micro-channel heat sink (a) exploded view of test module (b) dimensions of micro-channel heat sink (Unit: mm).

2.3. Procedure

In the flow boiling experiment, anhydrous ethanol of a purity of 99.8% was used as working liquid. Prior to conducting a test, the ethanol was circulated for 10 min to purge most gases in the flow loop. Subsequently, the flow rate and the inlet temperature were set to yield the desired test conditions by adjusting the flow rate and the temperature of water bath. Electrical power was then supplied to the cartridge heaters in the copper block in a small increment of 20–40 W. All the measurements of temperature were collected at steady-state which was considered to be achieved for each heat flux level when the mean temperature of the heat sink became constant (within 0.5 K fluctuations for at least 2 min). The inlet and outlet pressures were also recorded at each steady state.

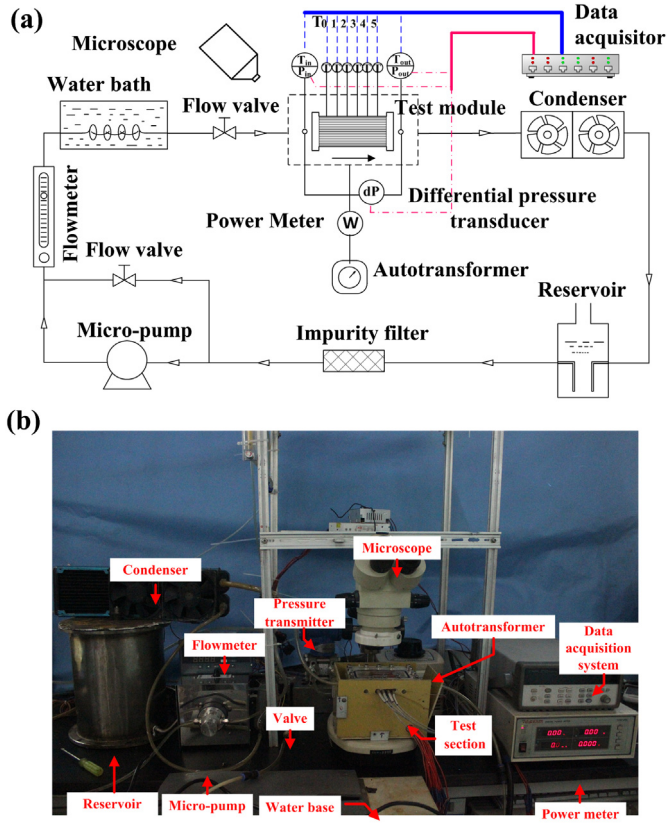

Fig. 3. Schematic of experimental setup and flow loop (a) schematic of the flow loop (b) photograph of main experimental apparatuses.

The collecting time of temperature and pressure data for each heat flux level was 5 min with a sampling frequency of 5 Hz.

2.4. Data reduction

2.4.1. Pressure drop

The pressure drop in the microchannels was defined as

$$\Delta P = (P_{in} - P_{out}) - P_{loss} \quad (1)$$

The values of inlet pressure, P_{in}, and outlet pressure, P_{out}, were the averages of the collection data during 5 minutes' acquisition time for each heat flux level.

Numerical simulation was employed to determine the pressure loss P_{loss} in the test section. The pressure distribution in a single unit cell under single-phase flow was simulated by using the commercial program of Fluent 6.3. The details of modeling are given in Fig. 4(a). The pressure drop in the unit cell was calculated using a simple force balance between shear force and pressure drop force. The simulation results shown in Fig. 4(b) imply that the pressure loss induced by the input and output manifolds is lower than 5% of the total pressure drop under both boundary conditions. In this study, the pressure loss was reflected in the uncertainty of pressure drop.

The fluctuation amplitudes of ΔP were obtained from the statistics of the real-time pressure data recorded by the data acquisition system. The upper and lower limits of ΔP fluctuation amplitude were evaluated by the average of the highest 20% ΔP values and the average of the lowest 20% ΔP values, respectively.

2.4.2. Mass flux

The mass flux, m, at the inlet of test section was calculated as

$$m = V\rho/A \quad (2)$$

Where V is the volumetric flow rate, ρ is the fluid density, and A is the overall cross-section of the microchannels.

2.4.3. Heat flux

With the assumption that the heating power distributes uniformly on the test heat sinks during this experimental study, the heat flux transferred to the fluid, named effective heat flux, was defined as

$$q = (N - N_{loss})/F \quad (3)$$

where N is the external heating power supplied by two cartridge heaters, F is defined as the plate area of the heater which is

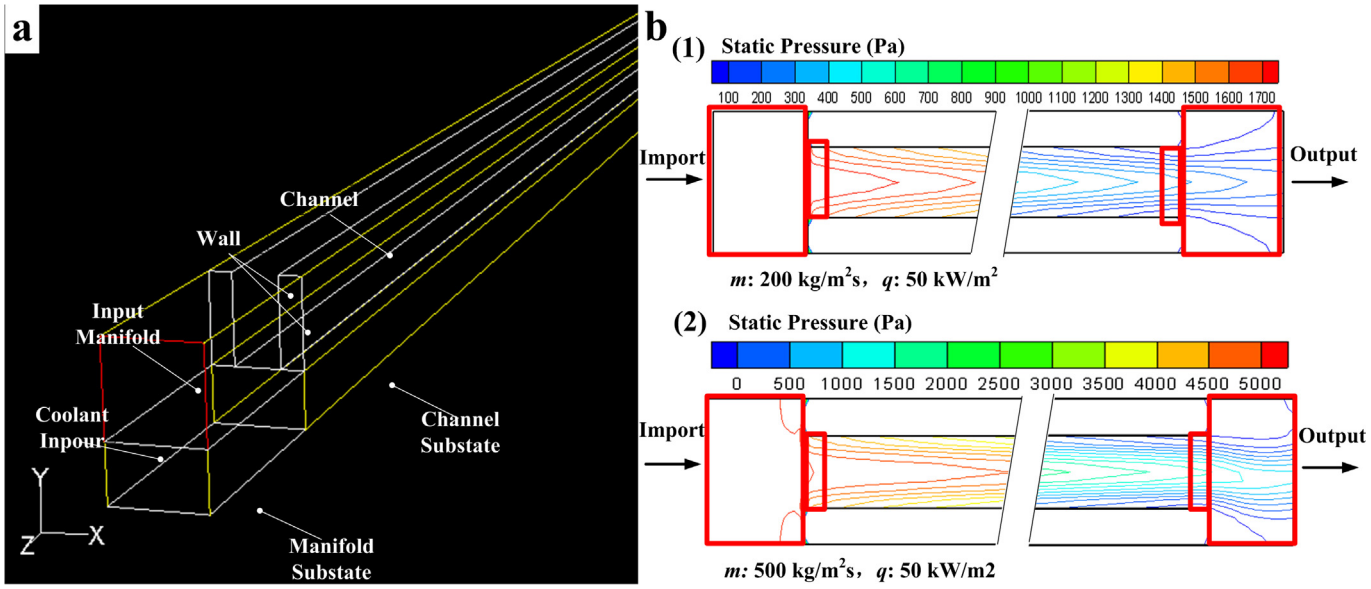

Fig. 4. (a) The model of simulated unit cell (b) pressure contour in the simulated unit cell.

32 × 10.8 mm in the experiment, N_{loss} is the heat loss due to conduction, convection and radiation. Based on the total heat balance of the test section, the heat loss was estimated by comparing the electric heat input with the actual heat transfer rate in terms of enthalpy difference between the inlet and outlet of the working fluid.

2.4.4. Heat transfer coefficient

Since the boiling heat transfer occurs only in the downstream channel, the single-phase flow region and two-phase flow boiling region coexist in a single channel. The study on the local heat transfer characteristic of test heat sink is needed for the better understanding of the heat exchange properties of solid-flow interface in micro-channels. The study of local flow boiling in the microchannels was defined at the 5th temperature measurement point from the inlet, where may be expected to remain well-developed flow boiling and avoid the effects from outlet manifold the tests. The assumption of thermal equilibrium was used to calculate the heat transfer coefficient in the boiling regime. The local two-phase flow heat transfer coefficient h_{tp} can be expressed by

$$h_{tp} = q/(T_{wi} - T_{sati}) \tag{4}$$

where q is effective heat flux, T_{wi} is the local wall temperature of the heat sink, and T_{sati} is the saturation temperature of local working fluid.

By assuming one-dimensional heat conduction between thermocouple location and channel bottom wall, the local wall temperature T_{wi} was evaluated by

$$T_{wi} = T_i - ql/K_s \tag{5}$$

where i is the sequence number of temperature measurement points, T_i is the measured temperature of the i-th measurement point (T_4 in this study), K_s is the thermal conductivity of copper, and l is the distance between the measurement point and the bottom of the channel.

With the assumption that the pressure in the microchannels obeys linear distribution along the axial direction, a linear interpolation was employed to determine T_{sati}.

2.4.5. Mass vapor

The values of mass vapor quality were calculated from equation of change in the enthalpy of a liquid–vapor system during evaporation in the microchannels.

2.5. Uncertainties analysis

The temperature of the heating wall and working fluid was measured with an accuracy 0.5 K (95% confidence level). Uncertainty analysis was conducted based on the method proposed by Kline [17]. The experimental uncertainties for the measured and reduced parameters are listed in Table 1.

3. Results and discussion

3.1. Pressure drop characteristics and two-phase instability

The comparison of pressure drop performance of the bare and porous-coated microchannels is presented in Fig. 5. The data were recorded with the inlet temperature of 30 °C. It indicates that for each heat flux, the pressure drop is higher for the porous-coated surface compared to that of the bare surface and the difference increases with increasing mass velocity and heat flux. This difference in pressure drop may due to the increased shear stress with the porous-coated surfaces, which is brought about by increasing surface roughness and turbulence. Similar to the observation of Khanikar et al. [12], the porous-coated surfaces seem to be more sensitive to the change in mass flux than that of bare surface.

Table 1
Experimental uncertainties for the measured and reduced parameters.

Parameters	Uncertainties (maximum)
Cross-sectional area	±5.8%
Temperature	±0.5 °C
Static pressure	±0.15%
Pressure drop	±5.2%
Heating power	±2.5%
Vapor quality	±12%
Max flux	±6.1%
Heat flux	± 8.4%
Heat transfer coefficient	±14%

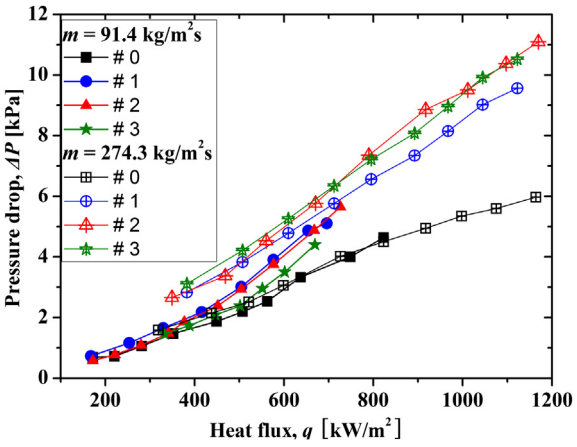

Fig. 5. Pressure drops versus the wall heat flux under different mass velocities for porous-coated and bare micro-channel heat sinks.

It shows that the increase of flow rate can lead to a higher pressure drop both in the bare and the porous-coated microchannels, especially at low heat flux region (<720 kW/m^2). The curves show sharp increase of pressure drop at particular heat fluxes, which can be explained by the onset of flow boiling. The pressure drop in the microchannels is highly depended on the bubble dynamics in the flow boiling region. The growth of large bubbles caused by the coalescence of plenty bubbles can be an explanation to the increase of pressure drop in the microchannels [18]. It indicates that the additional pressure drop caused by the introducing of porous coatings can be controlled within an acceptable range when a proper heat flux is selected (≤500 kW/m^2 for this case).

On the other hand, the susceptibility of flow boiling systems to the Ledinegg instability can be assessed by considering the negative segment of the pressure drop–mass flux gradient. As the slope $\partial(\Delta p)/\partial m$ becomes steeper, the system tends to exhibit static flow instability. A systematic study on the Ledinegg instability in microchannels has been presented by Zhang et al. [19]. The dynamic flow instability caused by pressure drop type oscillation will be the focus of our discussion below.

Fig. 6 presents the pressure drop transformation from single-phase to two-phase boiling flow for #0 and #1 at the mass velocity of 182.8 kg/m^{2}s. The average pressure drop of porous-coated surface shows a slight higher than that of bare surface. Notice that there is a significant jump of pressure drop for both samples with the upgrade of heat flux level. Meanwhile, the fluctuation of pressure drop is intensified, particularly for the bare microchannels. The two-phase flow dynamic instability may trigger the onset of CHF, and has been identified as a major concern in reliable operation of a microchannel heat exchanger. The bubble nucleation of the superheated liquid in microchannels may cause an explosive growth of the bubble, which expands in both downstream and upstream directions [4]. The bubble expansion upstream results in a back flow into the header of the parallel microchannels, which is a major source of instability in microchannels.

Fig. 7 indicates that the pressure drop fluctuation of microchannel is highly depended on mass flux and outlet vapor quality. Due to the limited heating power, the heat flux range studied in the flow boiling experiments was 200–1200 kW/m^2, which determined the outlet vapor quality was below 0.35. With the increase of outlet vapor quality, the bare surface shows sharp increase in pressure drop fluctuation while the porous-coated surface seems relatively steady. Moreover, the porous-coated microchannels show less sensitivity to the change of mass flux compared to that of bare surface.

Generally, a large fluctuation amplitude of flow pressure drop indicates a large force of the steam plume impacting to the flow channel. The erosion of the steam plume on the channel walls may cause the local drying, which leads to local temperature raising and heat transfer deterioration. Providing artificial nucleation sites, employing inlet restrictors, and incorporating heated regions to initiate nucleation are some of the remedies for the suppression of flow boiling oscillations in microchannels [5,20]. In this study, the significant improvement of flow boiling stability may be explained by the changes in bubble dynamics caused by introducing the porous coating layer. Many results of pool boiling studies show that porous coatings facilitate the nucleation process of bubbles and consequently lead to the great reduction of wall superheat. More importantly, the bubble dynamics on the porous surfaces show great differences compared to that on bare surfaces [14,21]. Kuo and Peles [22] demonstrated that the microchannels with structured surfaces were shown to promote nucleation of bubbles and to support significantly better reproducibility and uniformity of

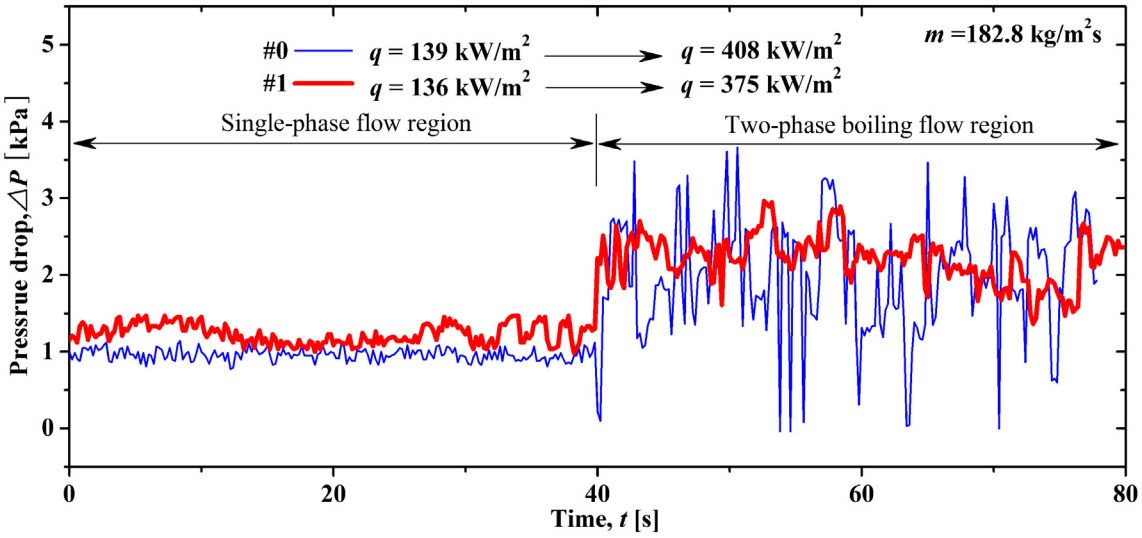

Fig. 6. Transient pressure drop of porous-coated and bare microchannels in different convective heat transfer zone.

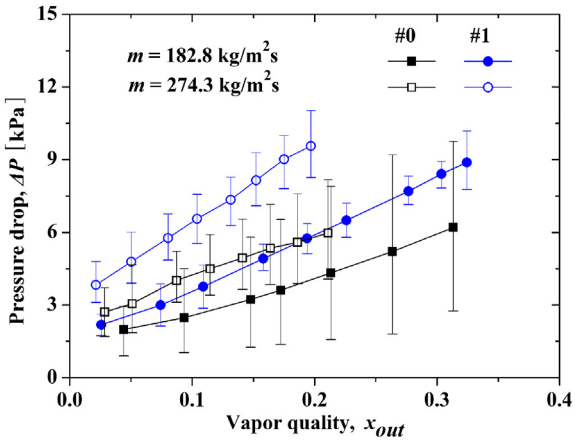

Fig. 7. Fluctuation amplitudes of pressure drop in porous-coated and bare micro-channels at different vapor qualities and mass flux.

bubble generation. The bubbles with much smaller departure diameter and higher departure frequency were observed in the porous-coated microchannels compared to those in bare micro-channels. The change in bubble dynamics can greatly reduce the probability of the formation of big bubbles which may expand in both downstream and upstream directions with the restriction of narrow flow channels and finally result in back flow. It is evident [23,24] that the enhanced structures enable a more orderly bubble nucleation process, and, to an extent, suppress the flow instability in microchannels. In addition, the increase of flow rate also reduces the coalescence of bubbles in flow channels.

3.2. Two-phase flow boiling heat transfer

Fig. 8 shows typical boiling curves of four samples obtained at the fifth thermocouple location. The data were recorded with the inlet temperature of 30 °C and flow rate of 182.8 kg/m^{2}s. It shows the slopes of all boiling curves are fairly constant at low heat fluxes corresponding to the single-phase flow regime. With the increase of heat flux, the slopes of the boiling curves show a sudden increase, which indicates the onset of flow boiling. The superheats at the phase transition points for case #1, #2 and #3 are apparently lower than that of case #0, which illustrates that the porous coatings in the micro-channels facilitate the onset of flow boiling. Griffith and Wallis [25] demonstrated that the geometry of a cavity containing trapped vapor is closely related to the bubble nucleation process. Under normal circumstances, the entrapped vapor and gas served as bubble embryos are much bigger than critical nucleation bubble [26] and may be uniformly superheated [27], which facilitates the activation of these nucleation sites. On the other hand, the separation of bubbles from the superheated boundary layer into the colder fluid volume is considerably impeded for the bare surface, which hinders the nucleation process [28]. Thus, the reduction of local wall superheat for the onset of nucleate boiling by the porous coatings can be well explained.

Fig. 9 shows dependence of the saturated flow boiling heat transfer coefficient on the thermodynamic equilibrium quality at the 5th temperature measurement point of the test section. The data were obtained at the mass flux of 182.8 kg/m^{2}s. The porous-coated samples (#1–#3) show great enhancement of heat transfer coefficient compared to that of bare sample (#0). However, the enhancement diminishes with the increase of vapor quality. Similar phenomenon was observed in the study on subcooled flow boiling in a small channel with diamond-particle microporous coating reported by Ammerman and You [29]. They attributed the diminishing of heat transfer enhancement to the adverse effect of the added conductive thermal resistance brought by the porous coating. Another possible explanation for the diminution of the boiling heat transfer enhancement is the change of heat transfer mechanisms resulted from the transformation of flow patterns [3,30]. With the increase of vapor quality, different flow patterns were observed in the porous-coated microchannels.

The effect of particle size on the heat transfer performance is given in Fig. 8. Cases #1 and #2 with smaller particle sizes (30 μm and 55 μm) exhibit better flow boiling heat transfer performance than that of case #3 with larger particle size (90 μm). The result is due to the higher heat transfer specific area and nucleation sites in porous media with smaller pore diameter [31]. Since the heat flux scope discussed in this study was limited to nucleate boiling regime, the highest heat transfer performance of case #2 may be explained by the most preferable bubble nucleation condition. As is known, it is difficult for liquid to penetrate into the porous layer with very small pores, which will thus fail to be activated at low heat fluxes. On the other hand, the large pores or cavities will be flooded by the subcooled liquid and unable to serve as stable nucleation sites. These adverse conditions will lead to higher superheats required for nucleation, and thereby hinder the enhancement. Sun et al. [32] suggested there is an optimum pore size for a given liquid in their study on the subcooled flow boiling heat transfer from microporous surfaces constructed by sintering spherical copper particles. In the present experimental range, 55 μm was considered the optimum particle diameter.

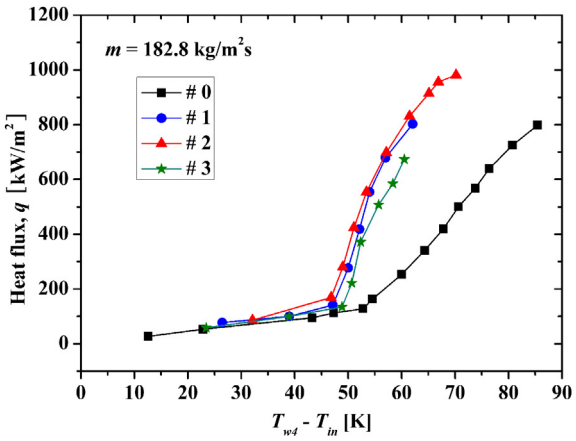

Fig. 8. Heat flux versus temperature difference between Tw_4 and T_{in} for porous-coated and bare micro-channel heat sinks.

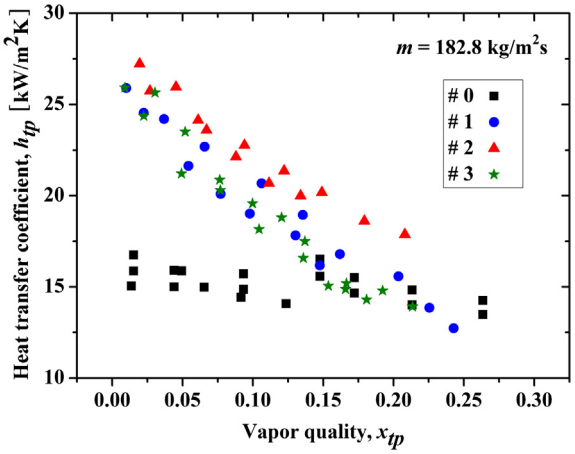

Fig. 9. Effect of vapor quality on heat transfer coefficient of porous-coated and bare micro-channel heat sinks.

4. Conclusion

In this study, the enhanced flow boiling of anhydrous ethanol in the porous-coated microchannels with hydraulic diameter of 540 μm was systematically investigated and compared to that in bare microchannels. Three heat sinks with porous-coated parallel microchannels were fabricated by using a solid-state sintering method. The copper particles used in samples #1, #2 and #3 were of about 30, 55 and 90 μm in diameter, respectively. The changes in pressure drop, flow boiling instability and flow boiling heat transfer performances caused by the introducing of porous coatings were discussed. The experimental results show that the introducing of porous coatings can lead to a slight higher pressure drop, and a significant mitigation of pressure drop fluctuation in the microchannels. The improvement in flow boiling stability can be explained by the changes in bubble dynamics and is highly depended on mass flux and outlet vapor quality. On the other hand, a dramatic enhancement of flow boiling heat transfer was obtained in the porous-coated microchannels, particularly at low vapor quality regime. The enhancement was due to the preferable bubble nucleation condition of porous coatings and diminished with the increase of vapor quality. Moreover, the flow boiling heat transfer performance of porous-coated microchannels showed dependence on particle size. In the present experimental range, the medium size of 55 μm was considered the optimum particle diameter.

Acknowledgements

The present research is sponsored by the direct fund of National Natural Science Foundation of China (No. 51146010) and the Doctoral research fund of Guangdong Natural Science Foundation (No. S2011040003189).

References

[1] D.B. Tuckerman, R.F.W. Pease, High-performance heat sinking for VLSI, IEEE Electron Device Letters EDL-2 (1981) 126–129.
[2] M.B. Bowers, I. Mudawar, High flux boiling in low flow rate, low pressure drop mini-channel and micro-channel heat sinks, International Journal of Heat and Mass Transfer 37 (1994) 321–332.
[3] G. Hetsroni, A. Mosyak, Z. Segal, E. Pogrebnyak, Two-phase flow patterns in parallel micro-channels, International Journal of Multiphase Flow 29 (2003) 341–360.
[4] S.G. Kandlikar, Heat transfer mechanisms during flow boiling in microchannels, Journal of Heat Transfer: Transactions of the ASME 126 (2004) 8–16.
[5] S.G. Kandlikar, W.K. Kuan, D.A. Willistein, J. Borrelli, Stabilization of flow boiling in microchannels using pressure drop elements and fabricated nucleation sites, Journal of Heat Transfer: Transactions of the ASME 128 (2006) 389–396.
[6] S. Krishnamurthy, Y. Peles, Flow boiling heat transfer on micro pin fins entrenched in a microchannel, Journal of Heat Transfer: Transactions of the ASME 132 (2010) 041007.
[7] S.G. Kandlikar, History, advances, and challenges in liquid flow and flow boiling heat transfer in microchannels: a critical review, Journal of Heat Transfer: Transactions of the ASME 134 (2012) 034001.
[8] R.L. Webb, The evolution of enhanced surface geometries for nucleate boiling, Heat Transfer Engineering 2 (1981) 46–69.
[9] I.L. Pioro, W. Rohsenow, S.S. Doerffer, Nucleate pool-boiling heat transfer. I: review of parametric effects of boiling surface, International Journal of Heat and Mass Transfer 47 (2004) 5033–5044.
[10] R. Wang, Y. Li, A. Gu, S. Hu, The experimental study of liquid nitrogen boiling heat transfer in vertical narrow channel of porous layer surface, Cryogenics 32 (Suppl. 1) (1992) 249–252.
[11] W. Wu, J.-H. Du, X.-J. Hu, B.-X. Wang, Pool boiling heat transfer and simplified one-dimensional model for prediction on coated porous surfaces with vapor channels, International Journal of Heat and Mass Transfer 45 (2002) 1117–1125.
[12] V. Khanikar, I. Mudawar, T. Fisher, Effects of carbon nanotube coating on flow boiling in a micro-channel, International Journal of Heat and Mass Transfer 52 (2009) 3805–3817.
[13] C.J. Kuo, Y. Peles, Flow boiling instabilities in microchannels and means for mitigation by reentrant cavities, Journal of Heat Transfer: Transactions of the ASME 130 (2008) 072402.
[14] J.P. O'Connor, S.M. You, A painting technique to enhance pool boiling heat transfer in saturated FC-72, Journal of Heat Transfer: Transactions of the ASME 117 (1995) 387–393.
[15] J.Y. Chang, S.M. You, Boiling heat transfer phenomena from microporous and porous surfaces in saturated FC-72, International Journal of Heat and Mass Transfer 40 (1997) 4437–4447.
[16] K.N. Rainey, S.M. You, Pool boiling heat transfer from plain and microporous, square pin-finned surfaces in saturated FC-72, Journal of Heat Transfer: Transactions of the ASME 122 (2000) 509–516.
[17] S.J. Kline, The purposes of uncertainty analysis, Journal of Fluids Engineering 107 (1985) 153–160.
[18] X.M. Dai, F.H. Yang, R.X. Fang, T. Yemame, J.A. Khan, C. Li, Enhanced single- and two-phase transport phenomena using flow separation in a microgap with copper woven mesh coatings, Applied Thermal Engineering 54 (2013) 281–288.
[19] T.J. Zhang, T. Tong, J.Y. Chang, Y. Peles, R. Prasher, M.K. Jensen, J.T. Wen, P. Phelan, Ledinegg instability in microchannels, International Journal of Heat and Mass Transfer 52 (2009) 5661–5674.
[20] A. Kosar, C.J. Kuo, Y. Peles, Suppression of boiling flow oscillations in parallel microchannels by inlet restrictors, Journal of Heat Transfer: Transactions of the ASME 128 (2006) 251–260.
[21] J.H. Kim, K.N. Rainey, S.M. You, J.Y. Pak, Mechanism of nucleate boiling heat transfer enhancement from microporous surfaces in saturated FC-72, Journal of Heat Transfer: Transactions of the ASME 124 (2002) 500–506.
[22] C.J. Kuo, Y. Peles, Local measurement of flow boiling in structured surface microchannels, International Journal of Heat and Mass Transfer 50 (2007) 4513–4526.
[23] A. Kosar, C.J. Kuo, Y. Peles, Boiling heat transfer in rectangular microchannels with reentrant cavities, International Journal of Heat and Mass Transfer 48 (2005) 4867–4886.
[24] C.J. Kuo, A. Kosar, Y. Peles, S. Virost, C. Mishra, M.K. Jensen, Bubble dynamics during boiling in enhanced surface microchannels, Journal of Microelectromechanical Systems 15 (2006) 1514–1527.
[25] P. Griffith, J.D. Wallis, The role of surface condition in nucleate boiling, Chemical Engineering Progress Symposium Series 49 (1960) 49–63.
[26] S.G. Bankoff, T. Haute, Ebullition from solid surfaces in the absence of a pre-existing gaseous phase, Journal of Heat Transfer: Transactions of the ASME 79 (1957) 735–740.
[27] N.H. Afgan, L.A. Jovic, S.A. Kovalev, V.A. Lenykov, Boiling heat transfer from surfaces with porous layers, International Journal of Heat and Mass Transfer 28 (1985) 415–422.
[28] Y.Y. Hsu, On the size range of active nucleation cavities on a heating surface, Journal of Heat Transfer: Transactions of the ASME 84 (1962) 207–216.
[29] C.N. Ammerman, S.M. You, Enhancing small-channel convective boiling performance using a microporous surface coating, Journal of Heat Transfer: Transactions of the ASME 123 (2001) 976–983.
[30] S. Saisorn, S. Wongwises, Flow pattern, void fraction and pressure drop of two-phase air–water flow in a horizontal circular micro-channel, Experimental Thermal and Fluid Science 32 (2008) 748–760.
[31] Z.Q. Chen, P. Cheng, T.S. Zhao, An experimental study of two phase flow and boiling heat transfer in bi-dispersed porous channels, International Communications in Heat and Mass Transfer 27 (2000) 293–302.
[32] Y. Sun, L. Zhang, H. Xu, X. Zhong, Subcooled flow boiling heat transfer from microporous surfaces in a small channel, International Journal of Thermal Sciences 50 (2011) 881–889.

Nomenclature

A: microchannel cross-section area (m^2)
D_h: hydraulic diameter (m)
F: plate area of the heater (m^2)
h_{tp}: local heat transfer coefficient (KW/m^2 K)
Ks: thermal conductivity of copper heat sink (KW/mK)
l: distance from thermocouple to bottom wall of microchannel (m)
P_{in}: inlet pressure (Kpa)
P_{loss}: pressure loss (Kpa)
P_{out}: outlet pressure (Kpa)
N: heating power (KW)
N_{loss}: heat loss (KW)
ΔP: pressure drop (KPa)
T_{sati}: saturated temperature of point i (K)
T_{out}: outlet temperature (K)
T_{wi}: thermocouple reading ($i = 0–5$) (K)
V: volumetric flow rate (m^3/s)
x_{out}: vapor quality
x_{tp}: local vapor quality
ρ: fluid density (Kg/m^3)

Subscripts
h: hydraulic
i: thermocouple i ($i = 0–5$)
in: inlet
out: outlet
q: heat flux (KW/m^2)
s: solid
t: time (s)
sat: saturation condition
T_{in}: inlet temperature (K)
tp: thermocouple position